Peer Community Journal

Section: Infections

Research article

Published
2024-02-28

Cite as
Moise S Kagbadouno, Modou Séré, Adeline Ségard, Abdoulaye Dansy Camara, Mamadou Camara, Bruno Bucheton, Jean-Mathieu Bart, Fabrice Courtin, Thierry De Meeûs and Sophie Ravel (2024) *Population genetics of* Glossina palpalis gambiensis *in the sleeping sickness focus of Boffa (Guinea) before and after eight years of vector control: no effect of control despite a significant decrease of human exposure to the disease*, Peer Community Journal, 4: e21.

Correspondence
thierry.demeeus@ird.fr

Peer-review
Peer reviewed and recommended by PCI Infections, https://doi.org/10.24072/pci.infections.100191

Population genetics of *Glossina palpalis gambiensis* in the sleeping sickness focus of Boffa (Guinea) before and after eight years of vector control: no effect of control despite a significant decrease of human exposure to the disease

Moise S Kagbadouno[1], Modou Séré[2], Adeline Ségard[3], Abdoulaye Dansy Camara[1], Mamadou Camara[1], Bruno Bucheton[3], Jean-Mathieu Bart[3], Fabrice Courtin[3,4], Thierry De Meeûs[#,3], and Sophie Ravel[#,3]

Volume 4 (2024), article e21

https://doi.org/10.24072/pcjournal.383

Abstract

Human African trypanosomosis (HAT), also known as sleeping sickness, is still a major concern in endemic countries. Its cyclical vector are biting insects of the genus *Glossina* or tsetse flies. In Guinea, the mangrove ecosystem contains the main HAT foci of Western Africa. There, the cyclical vector is *Glossina palpalis gambiensis*. A still ongoing vector control campaign (VCC) started in 2011 in the focus of Boffa, using tiny targets, with a 79% tsetse density reduction in 2016 and significant impact on the prevalence of the disease (from 0.3% in 2011 to 0.11% in 2013, 0.0352% in 2016 and 0.0097% in 2019). To assess the sustainability of these results, we have studied the impact of this VCC on the population biology of *G. p. gambiensis* in Boffa. We used the genotyping at 11 microsatellite markers and population genetic tools of tsetse flies from different sites and at different dates before and after the beginning of the VCC. In variance with a significant impact of VCC on the apparent densities of flies captured in the traps deployed, the global population of *G. p. gambiensis* displayed no variation of the sex-ratio, no genetic signature of control, and behaved as a very large population occupying the entire zone. This implies that targets deployment efficiently protected the human populations locally, but did not impact tsetse flies where targets cannot be deployed and where the main tsetse population exploits available resources. We thus recommend the pursuit of vector control measures with the same strategy, through the joint effect of VCC and medical surveys and treatments, in order to protect human populations from HAT infections until the disease can be considered as entirely eradicated from the focus.

[1]Programme National de Lutte contre la THA, Ministère de la Santé, Conakry, Guinée, [2]University of Dédougou, Dédougou B.P. 176, Burkina Faso, [3]INTERTRYP, Univ Montpellier, Cirad, IRD, Montpellier, France, [4]Représentation de l'IRD au Burkina Faso, 668, avenue du Pr Joseph Ki-Zerbo-Koulouba, 01 BP 182 Ouagadougou 01, Burkina Faso, [#]Equal contribution

Peer Community Journal is a member of the Centre Mersenne for Open Scientific Publishing
http://www.centre-mersenne.org/

e-ISSN 2804-3871

Introduction

Human African trypanosomosis (HAT), also known as sleeping sickness, is still a major concern for the WHO (Holmes, 2014; Simarro et al., 2015). Its agent is an euglenozoan kinetoplastid parasite, *Trypanosoma brucei gambiense* 1 (Jamonneau et al., 2019) (Tbg1), with a clonal propagation (Koffi et al., 2009, 2015), which recently emerged 10,000 years ago and spread from West Africa (Weir et al., 2016). It encompasses a complex life cycle, with a phase in blood sucking insects of the genus *Glossina* (Diptera, Hippoboscoidea), its cyclical vector (Bouyer et al., 2015).

In Guinea, the mangrove ecosystem still contains the main HAT foci of Western Africa (Simarro et al., 2015). There, *Glossina palpalis gambiensis* is the only known vector of the disease (Courtin et al., 2015). In Boffa, one of the three active HAT foci of the country (Kagbadouno et al., 2012), an active vector control campaign (VCC), aiming at reducing the human/tsetse contact, and subsequently at interrupting the transmission of Tbg1, was implemented in 2011 on the East bank of the Pongo river (Courtin et al., 2015). It is still ongoing and was extended to the whole focus in 2016 (Camara et al., 2021). This VCC was clearly successful, with a 80% reduction in individual catch per day, a 75% reduction of human exposure to tsetse bites, and a 70% reduction of the prevalence of the disease in the East bank of the Pongo river before 2016 (Courtin et al., 2015). Since 2016, for the whole focus, number of HAT cases dropped from 0.0352% to 0.0097% in 2019 (Camara et al., 2021). As regard to the vertebrate host, the exact role of animal or asymptomatic human reservoirs is still uncertain. Nevertheless, the genetic diversity of this parasite maintained by the Guinean populations suggests the existence of a significant amount of clonal lineages outside the patients involved in surveys (Koffi et al., 2009), in human and/or animal reservoirs. Several other studies appeared to confirm this hypothesis (Bucheton et al., 2002; Büscher et al., 2018).

A recent study of *G. palpalis palpalis* in the focus of Bonon (Côte d'Ivoire), revealed that a special allele at a given trinucleotide locus (GPCAG), experienced a brutal increase in frequency after control (Berté et al., 2019). This suggested the selection for resistance against control measure, associated with this particular allele.

Given these observations, deciding what strategies to use in the future will depend on the most precise knowledge we can get on the population impact of medical campaigns and VCC.

In this paper, we investigated the impact of VCC over 11 years on the HAT focus of Boffa (Figure 1), on capture densities and sex-ratio, as well as on *G. palpalis gambiensis* population genetics, in particular on locus GPCAG. We then discuss the best strategy to be used to optimize the protection of human populations from this neglected tropical disease.

Material and Methods

Data collection

All sites used for the entomological survey, number of captured flies and their gender can be seen in Kagbadouno et al (2012), Courtin et al. (2015), Camara et al. (2021), and, for most recent captures, in Supplementary file S1. All data and description of VCC in Boffa are available in two papers (Courtin et al., 2015; Camara et al., 2021) and the associated supplementary files of these articles.

Localization, date of sampling and number of genotyped flies can be found in Figure 1 and Table 1. A total of 290 flies were genotyped at 11 loci. Vector control was implemented with tiny targets from February 2012 in the sites of the left bank of Rio Pongo river and then on both sides after 2016. Then, according to Table 1, flies from 2009 and 2011 samples correspond to T0 (before control) on both sides of Rio Pongo river, while samples from 2019 and 2020 correspond to TX (after control has begun), on both sides of the river.

Active surveillance began in 2011, where 2730 individuals (1474 females and 1256 males) were captured. In 2019, 143 flies (80 females and 63 males) and in 2020, 215 (106 females and 109 males) were caught. The details on number of flies in the different dates and locations, and all genotypes, are available in the supplementary file S1.

Table 1 - Number of genotyped *Glossina palpalis gambiensis* (*N*) in the different traps of different sites and date of capture in the HAT Focus of Boffa (Guinea). The cohort (considering six generations of tsetse flies per year) and the time (T) after the beginning of control in months (0=before), the bank of the Rio Pongo river (see Figure 1) and the land type are also indicated.

Site	Trap	Date	Cohort	T	Bank	Land	*N*	N C-T-Bank
Guiapet	4	10/2009	0	0	Left	Island	23	C0-T0-LeftBank
Yangoya	1	10/2009	0	0	Left	Island	30	53
Bakyia	1	05/2011	10	0	Left	Continent	11	
Bakyia	2	05/2011	10	0	Left	Continent	8	
Bakyia	3	05/2011	10	0	Left	Continent	5	
Guiapet	2	05/2011	10	0	Left	Island	7	
Guiapet	3	05/2011	10	0	Left	Island	4	C10-T0-LeftBank
Yangoya	1	05/2011	10	0	Left	Island	7	65
Yangoya	5	05/2011	10	0	Left	Island	3	
Yangoya	6	05/2011	10	0	Left	Island	2	
Yangoya	7	05/2011	10	0	Left	Island	16	
Yangoya	8	05/2011	10	0	Left	Island	2	
Dobire	6	05/2011	10	0	Right	Island	20	
Dobire	7	05/2011	10	0	Right	Island	12	
Santani	2	05/2011	10	0	Right	Continent	10	C10-T0-RightBank
Santani	4	05/2011	10	0	Right	Continent	4	66
Santani	5	05/2011	10	0	Right	Continent	20	
Bakyia	2	10/2019	60	92	Left	Continent	4	
Guiapet	2	10/2019	60	92	Left	Island	2	
Guiapet	3	10/2019	60	92	Left	Island	11	
Yangoya	1	11/2019	60	93	Left	Island	2	C60-TX-LeftBank
Yangoya	5	11/2019	60	93	Left	Island	4	35
Yangoya	6	11/2019	60	93	Left	Island	1	
Yangoya	7	11/2019	60	93	Left	Island	11	
Dobire	6	11/2019	60	33	Right	Island	9	
Dobire	7	10/2019	60	32	Right	Island	1	
Santani	2	11/2019	60	33	Right	Continent	8	C60-TX-RightBank
Santani	4	11/2019	60	33	Right	Continent	1	27
Santani	5	11/2019	60	33	Right	Continent	8	
Bakyia	2	10/2020	66	104	Left	Continent	3	
Guiapet	1	10/2020	66	104	Left	Island	15	C66-TX-LeftBank
Guiapet	2	10/2020	66	104	Left	Island	1	24
Yangoya	7	10/2020	66	104	Left	Island	5	
Dobire	1	10/2020	66	44	Right	Island	6	
Dobire	5	10/2020	66	44	Right	Island	2	C66-TX-RightBank
Santani	1	10/2020	66	44	Right	Continent	10	20
Santani	3	10/2020	66	44	Right	Continent	2	

N C-T-Bank: Names and numbers of riverbank subsamples, with the cohort (C) and the time (T) before (0) or after (X) the beginning of control.

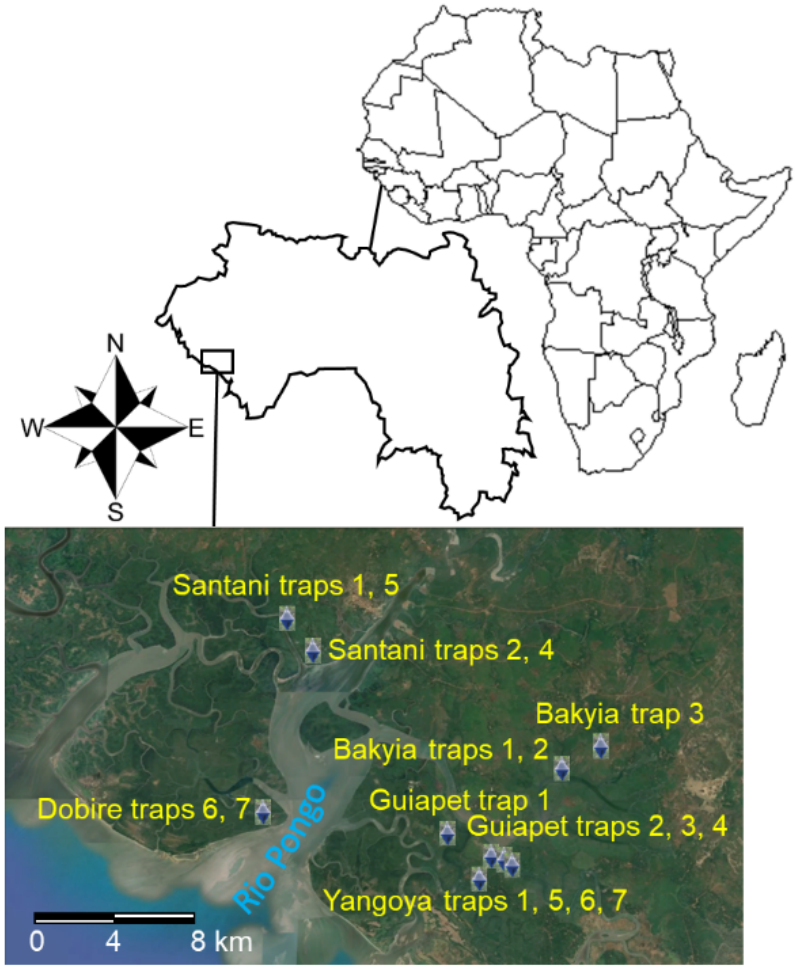

Figure 1 - Localization of traps for the capture of *Glossina palpalis gambiensis* in the HAT focus of Boffa in Guinea. Dates of capture, number of flies genotyped, and other geographical information can be found in the Table 1.

Assuming a two month generation time (Williams, 1990), as can be seen from Table 1, the genotyped subsamples extended from cohort 0 (2009), 10 (2011), 60 (2019) and 66 (2020). Because individuals belonging to one of these cohorts have no chance of interacting with any individual from another of these cohorts, we then always considered these four cohorts as belonging to distinct subsamples.

Homogeneity of sex-ratio was tested across cohorts with a Fisher exact test with Rcmdr.

Genotyping

Three legs of each tsetse fly were subjected to chelex treatment to obtain DNA for genotyping (Ravel et al., 2007). Genotyping was undertaken for 11 loci: X55-3 (Solano et al., 1997), XpGp13, pGp24 (Luna et al., 2001), GPCAG (Baker & Krafsur, 2001), pGp15, pGp16, and pGp27 (Ravel et al., 2020). Loci A10, B3, XB104, C102 were kindly provided by A. Robinson (Insect Pest Control Sub-program, Joint Food and Agriculture Organization of the United Nations/International Atomic Energy Agency Program of Nuclear Techniques in Food and Agriculture). Despite used at several occasions (Camara et al., 2006; Bouyer et al., 2007; Solano et al., 2009; Melachio et al., 2011), information about these loci were never published. Readers will find this information in Table A1 in the Appendix. Locus name with an X means that the locus is located on the X chromosome, and thus haploid in males. Cells with a “0” correspond to individuals with no amplification at the concerned locus, while uninterpretable profiles were coded “NA” (see Supplementary file S1).

Data analyzed

Genotyping was undertaken in different ways and under different conditions for the different dates of sampling (see Table S1). For samples collected in 2009 and 2011, allele bands were resolved on a 4300 DNA Analysis System (LICOR, Lincoln, NE) using two infrared dyes (700 and 800nm) as described in (Solano et al., 2009). For samples collected in 2019 and 2020, an ABI 3500xl sequencer (Applied Biosystem, Waltham, Massachusetts) was used with four different dyes (FAM, NED, VIC and PET) as described in Berté et al. (2019). Consequently, the 11 loci were not analyzed with the same dyes between samples from 2009-2011 and samples from 2019-2020. Because it is generally admitted that the dye used can modify the apparent size of the amplified alleles, we genotyped again some samples from 2009-2011 at the different loci using the ABI 3500xl sequencer to recode all the genotypes from the samples from 2009-2011. In some subsets, too many missing data were observed at some loci or subsamples. Consequently, to avoid multiple analyses, and to keep a reasonable number of loci and for the sake of consistency, population genetic analyses were undertaken with females only, at the eight loci that were successfully amplified over all the dataset (see Table S1): X55-3, XpGp13, pGp24, A10, B3, XB104, C102, and GPCAG.

Unless specified otherwise, the global dataset (File S1) was processed with Create (Coombs et al., 2008) to produce datasets in different formats, depending on the kind of analyses to be undertaken.

Selection of the relevant subsample units

The reproductive system of a population from a genotyped sample can be assessed through Wright's F_{IS} (Wright, 1965), which is a measure of the relative inbreeding of individuals as compared to the subpopulation they belong to. This parameter was estimated with Weir and Cockerham's unbiased estimator *f* (Weir & Cockerham, 1984), that we kept labelling F_{IS} for the sake of simplicity. In case of random mating in a dioecious population, a negative value is expected (Robertson, 1965; Pudovkin et al., 1996; Balloux, 2004; De Meeûs & Noûs, 2023). In tsetse flies, the trap can be the unit at which a significant subdivision may occur (Ravel et al., 2023), including *G. palpalis gambiensis* (Bouyer et al., 2009). Here, traps, and even sites, in combination with the cohort, often contained very few flies. To determine if traps, sites or river banks (right or left of the Rio Pongo River, see Figure 1) really mattered, we used the Wahlund effect approach (Goudet et al., 1994; De Meeûs et al., 2006). We compared the F_{IS_T} in traps, the F_{IS_S} in sites (ignoring traps), the F_{IS_B} within the two riverbanks (ignoring sites), and the F_{IS_C} within the four cohorts (0, 10, 61 and 67) (ignoring river banks). For this, we undertook a Friedman two-way analysis of variance by ranks for data paired by locus with the package R-commander (Fox, 2005, 2007) (rcmdr) for R (R-Core-Team, 2022). We then undertook planned one sided Wilcoxon signed rank test for paired data. If traps and/or sites and/or river banks matter, we expect a Wahlund effect (De Meeûs et al., 2007; De Meeûs, 2018) when pooling individuals from different origins (traps, and/or sites and/or river banks of the same cohort), meaning that the alternative hypothesis was $F_{IS\_T} < F_{IS\_S} < F_{IS\_B} < F_{IS\_C}$. When necessary (significant *p*-values), we corrected the *p*-values with the Benjamini and Yekutieli correction (Benjamini & Yekutieli, 2001) with R (command "p.adjust"), for test series with dependency.

Quality testing of loci and subsamples

Quality testing of the subsamples and genotyping was assessed with linkage disequilibrium (LD), Wright's F_{IS} and F_{ST} (Wright, 1965) and their variance across loci.

Linkage disequilibrium was tested with the *G*-based randomization test between each locus pair across subsamples as described in De Meeûs et al. (2009), with 10,000 random shuffling of genotypes of the two loci of each pair. Because there are as many non-independent tests as locus pairs, we adjusted the *p*-values with the Benjamini and Yekutieli (BY) procedure with R (command "p.adjust").

Wright *F*-statistics were estimated with Weir and Cockerham's unbiased estimators (Weir & Cockerham, 1984): *f* for F_{IS}, θ for F_{ST} and *F* for F_{IT}. Their significant deviation from the expected value under the null hypothesis (H0: $F_{IS}=0$ or $F_{ST}=0$) was tested with 10,000 randomizations of alleles between individuals within subsamples (for F_{IS}) and of individuals between subsamples (for F_{ST}). For F_{IS}, the statistic used was Weir and Cockerham's *f* for each locus and overall. For testing subdivision we used the *G*-based test (Goudet et al., 1996) for each locus and overall. For F_{IS}, tests were one-sided ($F_{IS}>0$), and two-sided *p*-values were obtained by doubling the one-sided *p*-value if <0.5 or we doubled 1-*p*-value otherwise. Confidence intervals (95%CI) were computed with 5000 bootstraps over loci for the average over loci, and

over individuals for the confidence intervals around each locus. The standard error of jackknives over loci (SE) was computed for F_{IS} and F_{ST} (SE_F_{IS} and SE_F_{ST} respectively) for null allele diagnostics (see below).

All this computations and randomizations were undertaken with Fstat 2.9.4 (Goudet, 2003), updated from Fstat 1.2 (Goudet, 1995), except the bootstraps over individuals, for which we used Genetix (Belkhir et al., 2004). Since Genetix computes bootstraps for each locus in each subsamples, we averaged these values across subsamples to obtain 95%CI of F_{IS} for each locus.

Null allele signatures were looked for with several criterions: the ratio of SE of F_{IS} over F_{ST} (r_{SE}), as computed with jackknives over loci; the correlation between F_{IS} and F_{ST}, and between F_{IS} and the number of missing genotypes (N_b) (De Meeûs, 2018). These correlations were tested with a one-sided (positive correlation) Spearman's signed rank correlation test. The regression F_{IS}~N_b was also undertaken to determine the proportion of the variance of F_{IS} that was explained by missing genotypes (putative null homozygotes) with the determination coefficient R^2, and to extrapolate the possible basic F_{IS} (F_{IS_0}) in absence of null alleles through the intercept of this regression. Null allele frequencies were also estimated with the EM algorithm (Dempster et al., 1977) implemented by FreeNA (Chapuis & Estoup, 2007). For these analyses, missing genotypes (true blanks) were coded as null homozygotes for allele 999, as recommended (Chapuis & Estoup, 2007). The goodness of fit of observed blank genotypes, with the expected number of missing data, was assessed with a one-sided exact binomial test with R (command "binom.test"). If null alleles and random mating fully explain the data, there should be at least as many blank genotypes as expected. For this test we computed the square of null allele frequency of each locus in each subsample and multiplied it by the subsample size. To increase statistical power, we summed these expected number of null homozygotes over all subsamples ($N_{Exp\text{-}b}$) and compared those to the observed number of missing genotypes for each locus, over all the considered dataset. We then also undertook the regression F_{IS}~p_n, where p_n is the global null allele frequency.

Stuttering detection and correction followed the procedure described elsewhere (De Meeûs et al., 2021; De Meeûs & Noûs, 2022) over all subsamples and for each locus, using the associated template "TestStutterDioecious-n1000N100-1-10%Stuttering.xlsx" available on Zenodo (https://doi.org/10.5281/zenodo.8181166; Kagbadouno et al., 2023), exact binomial tests and adjustment of *p*-values with Benjamini and Hochberg (BH) procedure with R (command "p.adjust").

Short allele dominance (SAD) was looked for with the correlation method between F_{IT} and the size of the alleles (Manangwa et al., 2019) using a one-sided (negative relationship) Spearmans rank correlation test. In case of doubt, we also undertook the regression F_{IS}~Allele size, weighted with $p_i(1\text{-}p_i)$, and where p_i was the frequency of the allele (De Meeûs et al., 2004). Correlation and regression tests were undertaken with rcmdr (Fox, 2005, 2007). For SAD, the regression allows to minimize spurious correlations due to rare alleles. In rcmdr, regression tests are two-sided. To obtain a one-sided *p*-value, when the slope was negative, we simply halved the two-sided *p*-value, or computed 1-*p*-value/2 otherwise. We labelled the correlation *p*-value p_{cor} and the regression one p_{reg}.

Subdivision

Comparisons of *F*-statistics between different subsamples or between F_{IS} and F_{IT} was undertaken with Wilcoxon signed rank tests for paired data with rcmdr, using the loci as pairing factor. Tests were one-sided in the appropriate direction (e.g. F_{IT}>F_{IS}). Subdivision was measured and tested with Wright's F_{ST} and the *G* randomization test, as described above. Genetic differentiation was measured and tested between each pair of cohorts in the same way, except that systematic paired test required BY corrections for significant *p*-values.

Effective population sizes and effective population densities

We estimated effective population sizes (N_e) with several algorithms and softwares. The first method is the heterozygote excess method from De Meeûs and Noûs (De Meeûs & Noûs, 2023), computed for each locus in each cohort, ignoring values below or equal to 0, and averaged across loci, for each subsample (e.g. cohort). The second method was the linkage disequilibrium based method (Waples & Do, 2010), corrected for missing data (Peel et al., 2013), implemented by NeEstimator (Do et al., 2014), and assuming random mating and selecting results for alleles with frequency above or equal to 5%. The third method was the co-ancestry method (Nomura, 2008), also implemented by NeEstimator. The fourth method used the averages obtained with four temporal methods. Three were implemented in NeEstimator: Pollak, Nei and Tajima,

and Jorde and Ryman (Nei & Tajima, 1981; Pollak, 1983; Jorde & Ryman, 2007) assuming random mating and selecting results for alleles with frequency above or equal to 5%. For these three temporal method, we averaged N_e across the different comparisons (different cohort pairs), ignoring "Infinite" outputs. The last temporal method was the maximum likelihood temporal method implemented in MLNe (Wang & Whitlock, 2003). For MLNe, maximum and minimum values corresponded to the confidence interval outputted by the procedure. We then computed the average across all temporal methods, weighted by the number of usable values and averaged minimum and maximum values in the same way. For MLNe, the weight was the number of cohort pairs (6). The fifth method was the within and between loci identity probabilities (Vitalis & Couvet, 2001a) with Estim (Vitalis & Couvet, 2001b). The sixth method was the sibship frequency method (Wang, 2009) with Colony (Jones & Wang, 2010), assuming female and male polygamy, and inbreeding. For each method, we computed the average, the minimum and maximum across usable values, and assigned a weight (number of usable values). For temporal methods, the weight was set to 4 (number of cohorts). We then obtained the grand average for N_e and minimum and maximum (minimax) values through an average across methods, weighted by the aforementioned weights. This methodology obviously provided a rough approximation of N_e and the space of its possible values, and finding the most accurate way will need specific multi-scenarios simulation approaches, as discussed elsewhere (De Meeûs & Noûs, 2023).

To compute effective population densities, we considered three different surfaces, computed with the function "insert a polygon" of Google Earth Pro. The smallest area was defined by the traps containing flies that were indeed genotyped, as in Figure 1 and Table 1, and labelled S_{Genet}=132 km². The second surface was defined by all traps that captured at least one tsetse fly in 2011, during the most extensive survey campaign (Kagbadouno et al., 2012) (see File S1), S_C=224 km². The third area was defined by the limits of the survey defined before 2011 (see File S1); S_L=629 km². The largest surface was drawn considering all "mangrove-like" environments in Google Earth Pro, S_{max}=1301 km². Effective population densities were then computed by dividing the effective population size by these surfaces. For the sake of comparison, we also computed the densities of captured flies in 2011 (initial survey, T0), in 2019 and 2020 (see Files S1 for raw data). We also compute the sex-ratios of captured (C) flies, $SR=N_{c\text{-}males}/N_{c\text{-}females}$ with these data. The homogeneity of the proportion of females across cohorts was tested with a Fisher exact test with rcmdr. The evenness of sex-ratios was then tested with a two-sided exact binomial test with R (command "binom.test").

Finally, maximum distances between the most remote sites defined by each aforementioned surface was computed with Google Earth Pro with the menu "Add a trajectory".

Bottleneck signatures

We tried to find bottleneck signatures with the diversity excess method and the Wilcoxon signed rank test method with Bottleneck (Cornuet & Luikart, 1996), with a particular interest to subsamples genotyped after the beginning of control (cohorts 61 and 67). We used the three mutation models: IAM, TPM with default options, and SMM. Significant signatures of a bottleneck can be suspected if the test is highly significant with the IAM and significant with the TPM at least. Weaker signals tend to be produced in population with very small effective population sizes (De Meeûs, unpublished simulation results).

Results

Captured flies, apparent densities and sex-ratio

The number of flies captured, per gender and total, the apparent density per trap and day (ADTD) and the sex-ratio for the different cohorts are presented in Table 2. There is a clear drop in ADTP after the beginning of VCC. We also observed a significant change in sex-ratio across cohorts (p-value=0.0015), but this is only due to the small sex-ratio observed in 2009 (Table 2). When we removed 2009 data, differences are not significant any more (P-value=0.491).

Defining the relevant geographic scales for subsample units

There was no significant difference between F_{IS_T}, F_{IS_S} and F_{IS_B} (all p-values>0.4) (Figure 2). We thus ignored traps, sites and river banks for further analyses, and kept only the different cohorts (cohorts 0, 10, 60 and 66) as subsample units.

Table 2 - Number of males (N_M), females (N_F) and total number (N) of *Glossina palpalis gambiensis* captured in the HAT focus of Boffa (Guinea), with year of capture and corresponding cohort, apparent density per trap and day (ADTD) and sex-ratio.

Year	Cohort	NM	NF	N	ADTD	Sex-ratio
2009	0	41	97	138	23.00	0.42
2011	10	1246	1484	2730	25.87	0.84
2019	60	62	82	144	4.44	0.76
2020	66	68	68	136	3.58	1

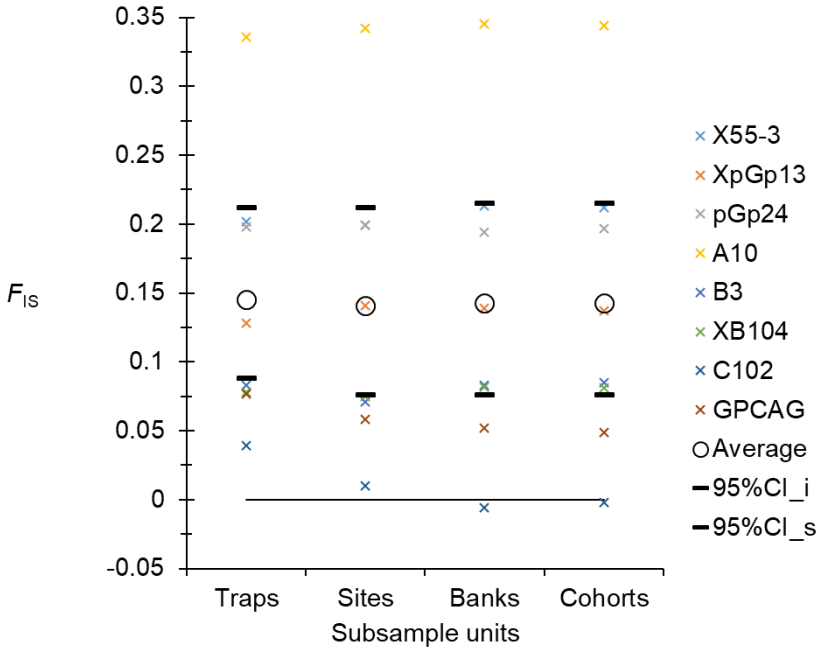

Figure 2 - Comparisons of F_{IS} within traps (F_{IS_T}), within sites (ignoring traps) (F_{IS_S}), within river banks (ignoring sites) (F_{IS_B}), and within each cohort (ignoring river banks) (F_{IS_C}) in female subsamples of *Glossina palpalis gambiensis* across 11 years in the mangroves of Boffa, Guinea, for eight loci (crosses of different colors), average (empty circles) and 95%CI (black dashes). The global comparison outputted a p-value=0.9663 and none of paired tests provided a p-value<0.4.

Quality testing of the subsamples and loci

Only one locus pair out of 28 appeared in significant LD (less than 4%) (p-value=0.039). It did not remain significant after BY correction. We thus considered all loci to be statistically independent from each other's.

There was a substantial but variable heterozygote deficit: F_{IS}= 0.143 in 95%CI=[0.076, 0.215] (p-value<0.0002) (Figure 3). With r_{SE}=19, and the positive correlation between F_{IS} and F_{ST} (ρ=0.5988, p-value=0.0584), we could suspect that most of this heterozygote deficit could be explained by null alleles. Nevertheless, the correlation between F_{IS} and N_b did not seem to confirm this (ρ=0.0952, p-value=0.4201). Nonetheless, this lack of signal resulted from three outlier loci (pGp24, B3 and C102), which displayed too many missing genotypes as regard to their relatively low F_{IS} (Figure 3). This means that many of these missing data, at these three loci, probably did not correspond to true null homozygotes.

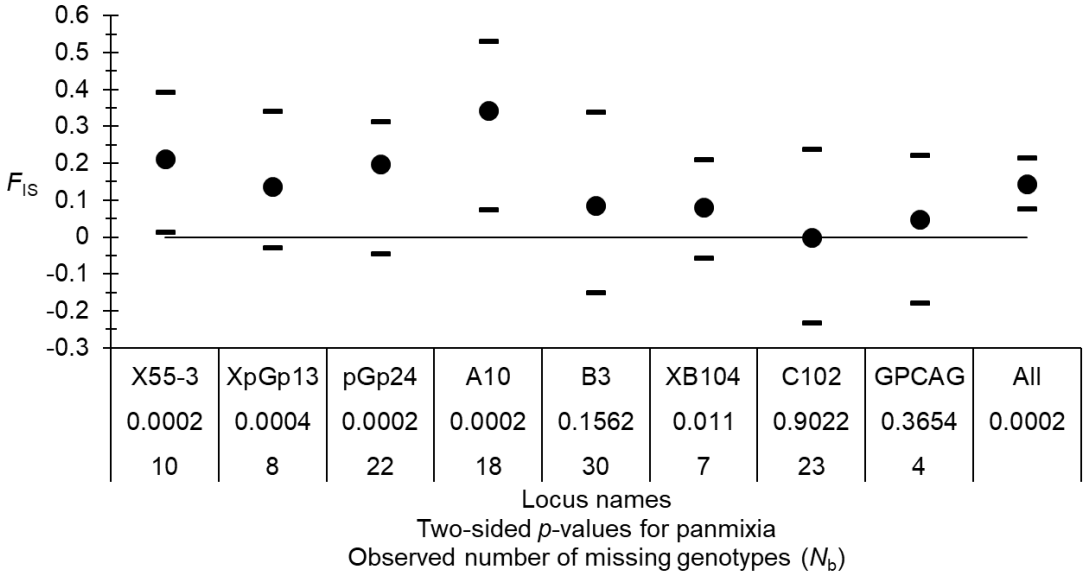

Figure 3 - Variation of F_{IS} across loci in the four cohorts of *Glossina palpalis gambiensis* from Boffa (Guinea). Averages (black dots), and 95% confidence intervals (black dashes) were computed by 5000 bootstraps over individuals (for each locus) and over loci (All). The two sided *p*-values for significant deviation from panmixia and the number of observed missing genotypes are also provided.

We thus undertook the correlation and the regression F_{IS}~N_b without these three loci. The results can be observed in the Figure 4. The correlation became significant and the regression suggested that missing genotypes (null alleles) explains almost all (96%) of F_{IS} variation. The intercept was negative, as expected in small, pangamic dioecious populations (F_{IS_0}=-0.0412 in 95%CI=[-0.1872, 0.1171]).

For null allele frequency estimates, we recoded as homozygous for the null allele (allele coded 999) all missing genotypes but for the three outlier loci. Indeed, for these loci, most missing data (coded "0", and kept as such) probably corresponded to another problem. With these data, estimate of null allele frequencies, and the resulting expected number of missing data over all subsamples fitted very well with the observed ones at each locus (all *p*-values>0.2). Moreover, the regression F_{IS}~p_n displayed very good results (R^2=0.8566, F_{IS_0}=0.012 in 95%CI=[-0.1951, 0.2143]). In this regression, loci pGp24, B3 and C102 were not outliers anymore. Nevertheless, the impossibility to determine which missing data are true null homozygotes at these loci provided a drop in accuracy. Without those, the regression was improved (R^2=0.9851, F_{IS_0}=-0.0391 in 95%CI=[-0.1891, 0.1151]).

We also undertook the stuttering and SAD analyses. We found a significant stuttering signature for locus A10 only (*p*-value=0.0286). Nevertheless, null alleles explained this locus well enough (Figures 3 and 4) so that we could consider this result as coincidental. Three loci displayed marginally significant or not significant signatures of SAD: X55-3 (p_{cor}=0.0423, p_{reg}=0.1551), pGp24 (p_{cor}=0.0963, p_{reg}=0.0489), and B3 (p_{cor}=0.288, p_{reg}=0.4841). Given the weakness of such results, and that these three loci were very well explained by null alleles, we did not consider that any locus was affected by SAD, and that a few null alleles randomly associated with small alleles provided these weak signatures.

We detected no Wahlund effect and the significant heterozygote deficits observed were entirely caused by null alleles of frequencies 0.02 to 0.28.

Average subdivision was globally not significant with a weak variance across the different loci: F_{ST}=-0.001 in 95%CI=[-0.004, 0.004] (*p*-value=0.6938). In particular, GPCAG displayed a negative value: F_{ST}=-0.007 (-0.006 with FreeNA correction) (*p*-value=0.1709), and allele 219 (here labelled 220, due to probable lag produced by the change in size calibration on this species), did not increase in frequency after control had begun: 0.094, 0.093, 0.065, and 0.022 for cohorts 0, 10, 60 and 66, respectively.

Subdivision

As demonstrated above, we could not detect any geographic subdivision signature. Subdivision was globally weak across the different cohorts: average F_{ST}=-0.001 in 95%CI=[-0.004, 0.004] and not significant

(p-value=0.6938). Moreover, F_{IT}=0.142 in 95%CI=[0.073, 0.218] was not significantly bigger than F_{IS}=0.143 in 95%CI=[0.076, 0.215] (p-value=0.7695).

We also measured and tested subdivision between each pair of cohorts. In the Figure 5, we can confirm the absence of any subdivision. Moreover, subdivision between cohorts before control (T0) and after control had begun (TX) did not appear bigger than for other cohort comparisons.

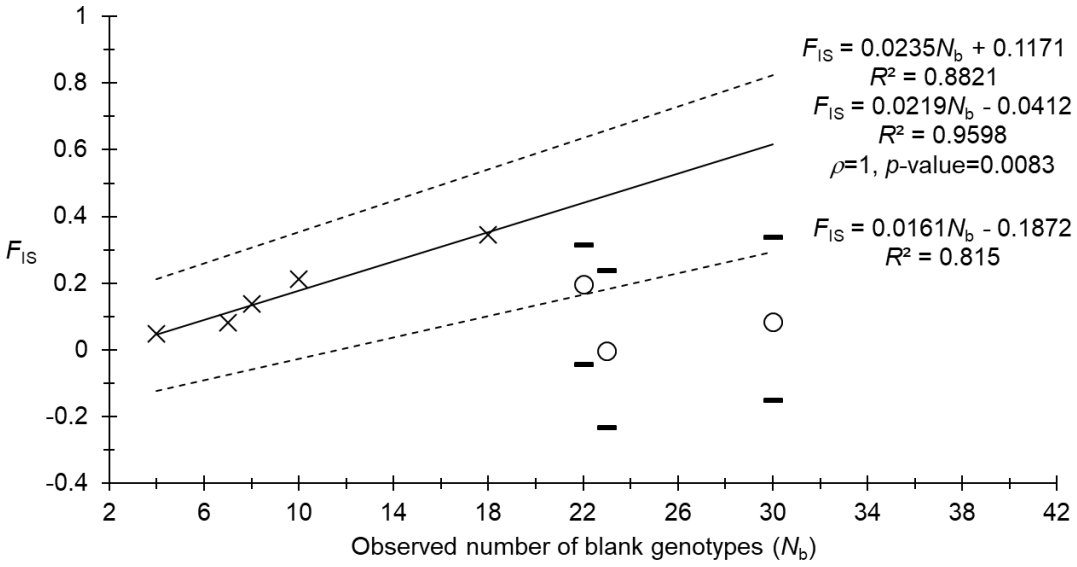

Figure 4 - Regression of F_{IS} by the number of missing genotypes (black crosses and continuous line) without loci displaying an excess of missing genotypes (pGp24, B3 and C102) (empty circles) and of the corresponding 95%CI of bootstraps over individuals for *Glossina palpalis gambiensis* from Boffa (Guinea) (black dashes and broken lines). Regression equations, the determination coefficient (R^2) and the result of the correlation test are also given.

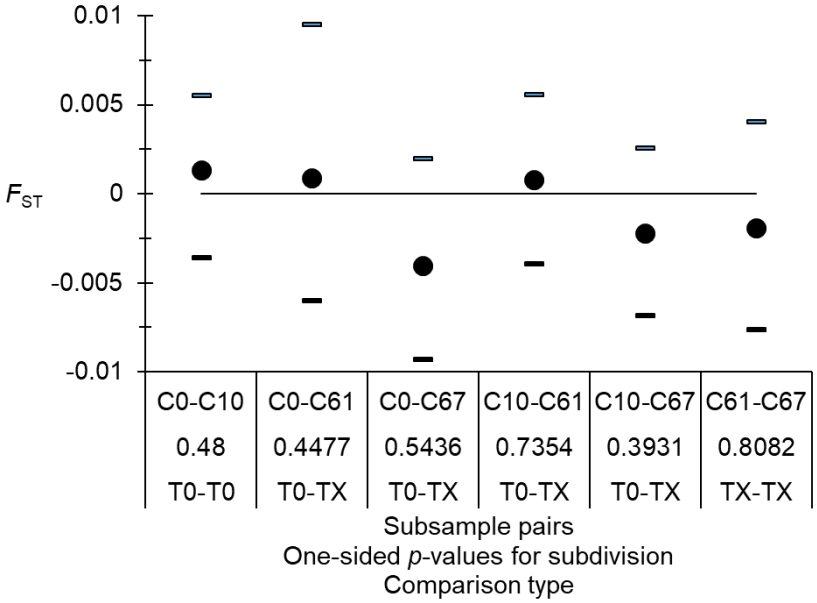

Figure 5 - Subdivision measures (F_{ST}) and test between each pair of cohorts (C0, C10, C60 and C66). The result of the test (p-values) and the comparison type between cohorts before control (T0) or after the beginning of control (TX) are also indicated.

Effective population sizes and effective population densities

For this section, Estim provided no usable values. For the remaining methods, results are presented in the Table 3 and Figure 6. These values were quite variable, but did not display particularly smaller values

after control (26 and 18 for cohorts 60 and 66 respectively) than before control (22 and 42 for cohorts 0 and 10 respectively). Nevertheless, such comparisons could only be made for the heterozygote excess, co-ancestries and sibships methods. The apparent increase in 2011 (cohort 10, before the VCC) can only be observed for three methods (heterozygote excess, Coancestries and Sibship). It is probably more due to sampling variances than to a real and brutal increase of the tsetse population.

Table 3 - Effective population size, minimum and maximum values estimated with different methods, and over all method (average weighted with "Weight"). Codes for methods are HzEs: heterozygote excess; LD: linkage disequilibrium; CoAn: coancestries.

	Methods					
	HzEs	**LD**	**CoAn**	**Temporal**	**Sibship**	**Over all**
Average	14	461	24	15130	44.5	3830
Minimum	5	461	21	404	32	143
Maximum	24	461	28	18957	73	4798
Weight	4	1	3	4	4	

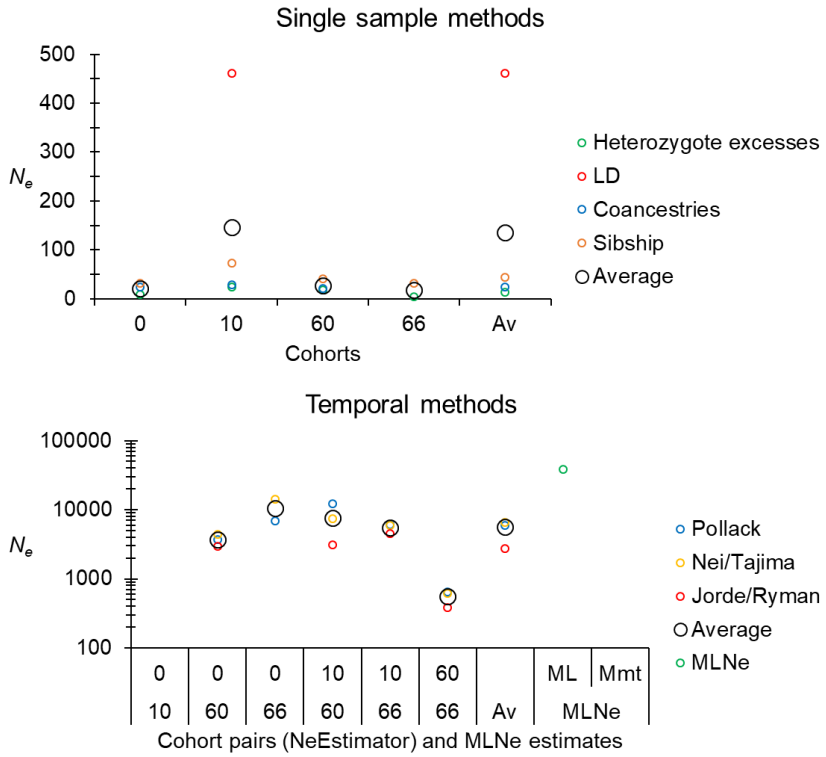

Figure 6 - Comparisons of effective population sizes obtained with the different single sample and temporal samples methods for *Glossina palpalis gambiensis* from the sleeping sickness focus of Boffa, for the different cohorts and cohort pairs and unweighted averages (Av) over those, and for temporal methods implemented in MLNe, over all cohorts. Empty data means "Infinite" result. ML: maximum likelihood; Mmt: moment.

Taking the surface occupied by genotyped flies, the resulting effective population density was $D_{e\text{-Genet}}$=8 in minimax=[1, 17] flies per km². However, given the absence of any population subdivision signature, we considered that this quantity was a very strong overestimate. In the Figure 7, we can see the effective population densities computed with S_C, S_L and S_{max}. Such densities became much smaller when temporal methods were ignored ($D_{e\text{-max}}$=0.05km² in minimax=[0.04, 0.06]).

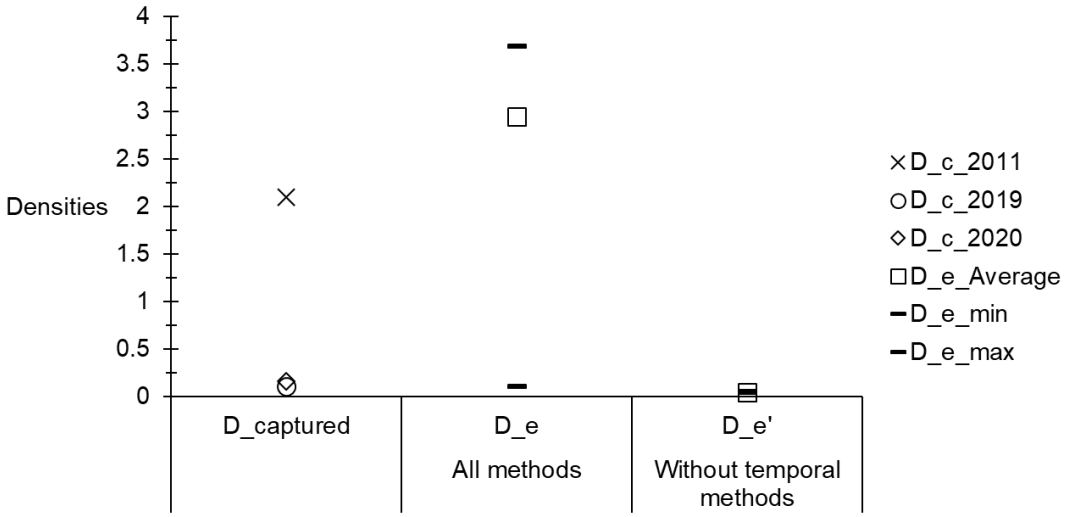

Figure 7 - Densities of captured flies (D_c) and corresponding effective population densities (D_e) while considering the whole surface of Boffa (as defined in the text) occupied by tsetse flies in the HAT focus of Boffa (Guinea), for different years and different effective population size averages: with all methods, or without temporal methods.

There was no significant variations of the sex ratio across years (0.85, 0.79 and 1.03 for 2011, 2019 and 2020 respectively) (p-value=0.3253). Combining all years, captured flies displayed a highly significant female biased sex ratio SR=0.86 (p-value<0.0001).

Capturing flies after control had begun, in the same trapping sites, obviously appeared more difficult than before control (Figure 7).

The maximum distances between the most remote points were 19 km, 40 km, 44 km and 62 km for the areas S_{Genet}, S_C, S_L and S_{max} respectively. Depending on the true area occupied by the population of tsetse flies in Boffa, these may represent the average dispersal distances from one generation to the next.

Bottleneck signatures

The results of these analyses are given in Table 4, where an absence of any bottleneck signature can be noticed, in particular after the beginning of control (cohorts 60 and 66).

Table 4 - One sided p-values for the detection of a genetic signature of a bottleneck with the three models of mutation (IAM, TPM and SMM) for the different subsamples before the beginning of vector control (Cohorts 0 and 10) and after the beginning of control (Cohorts 60 and 66).

Cohort	IAM	TPM	SMM
Cohort 0	0.3711	0.9629	0.9981
Cohort 10	0.6289	0.9980	1
Cohort 60	0.5781	0.9863	0.9961
Cohort 66	0.6289	0.6797	1

Discussion

All heterozygote deficits observed at the eight loci that passed the quality control tests were entirely explained by null alleles. Wahlund effect or inbred systems of mating were dismissed by different observations: absence of linkage disequilibrium; variance of F_{IS} across loci, with several ones not significantly deviating from the panmictic model; negative intercept of the regression F_{IS}~N_b. The eight loci studied here in female *G. palpalis gambiensis* converged with the existence of a large and stable pangamic population of this species occupying the HAT focus of Boffa. This was confirmed by the absence of any Wahlund effect when pooling all individuals from all the sampling area into one subsample in each cohort. The regression of the F_{IS} with null alleles or number of missing data, with a determination coefficient close

to unity and a negative intercept confirmed this perception. No notable difference in effective population sizes from one cohort to the other could be observed. The apparently increase in cohort 10, before the beginning of the VCC, was probably due to sampling variance. Indeed, it is quite unlikely that, as brutal it could have been, an increase in the size of the population would present a significant signature in its effective population size after only 10 generations. If so, it is then hard to understand why no signature of any bottleneck was observed at generation 66. We could not observe any genetic differentiation between the different cohorts, whether within or between dates before or after the VCC had begun. This was in line with the extreme effective population size estimates with temporal methods, as compared to single sample based methods. The reality probably lies in between, which means that some genetic drift should occur, leading to some genetic differentiation. This may require more autosomal markers to be confirmed.

Subdivision tests also confirmed a free migration of tsetse flies in the area defined by this tsetse population. Taking the total surface where flies could be captured and the total surface of the survey, as the most realistic values, the corresponding dispersal distance would be between 40 and 44 km per generation. The constant shading, high humidity and wind conditions of the particular continuously favorable mangrove ecosystem probably explain such important values (Courtin et al., 2010, 2015; Courtin & Kagbadouno, 2011). Within these surfaces, the effective population density could be considered to vary between 3 and 6 individuals per km², in minimax≈[0.1, 8]. These range within the smallest values as compared to what can be found elsewhere (De Meeûs et al., 2019). This is even worse if we consider that, here, we could use temporal methods for estimating effective population sizes. Temporal methods are almost never available in the literature, but provided very high values in the present study. Without temporal methods, densities would have fallen to very small values: between 0.05 and 0.1 individuals per km² only, for the two surfaces respectively.

We observed a significant female biased *SR* in this population with small effective population densities. In a recent study of *G. fuscipes fuscipes* from Chad (Ravel et al., 2023), authors found a negative correlation between *SR* and densities. Scattered distribution of hosts, leading to smaller effective population densities of the flies, would impose to these insects to travel more to find blood meals. Because of larval feeding, female tsetse would need to feed more often than males and be captured more often than those in such kind of ecological frameworks. On the contrary, abundance of hosts would maintain dense populations of tsetse flies, with no need to spend time seeking for blood meals, especially so for females, while males still need looking for mates.

We observed the absence of any significant genetic differentiation between subsamples before and after the beginning of control, especially at locus GPCAG. Additionally, we failed to evidence any strong (if any) effect on effective population sizes before and after the beginning of VCC, and observed a total absence of any genetic signature of a bottleneck, even after a 79% drop in captured flies (Camara et al., 2021). All these results testify of an absence of consequences of the VCC on the genetic structure of this tsetse population, at the scale of the focus. Nevertheless, the dramatic drop in captured flies after the VCC had begun, indicated an efficient protection of the human population against tsetse bites around the targeted zones. The drop in tsetse bites and HAT prevalence and incidence in selected controlled zones has already proved such a protection (Courtin et al., 2015). It also indicates that in the areas targeted by vector control, tsetse densities would probably regain initial levels rapidly in case of scaling back. The fact that a significant decrease in HAT prevalence was observed (Courtin et al., 2015; Camara et al., 2021) also advocates for the benefic effects of the VCC. Finally, the absence of impact on the targeted population at the scale of the whole mangrove of Boffa, suggests that VCC as it was undertaken, is efficient at protecting human populations, but does not significantly affect the genetic diversity of this particular system. “Emptied” spots simply became reinvaded by a representative sample of the whole population, which may come from any part of the focus, even locally. Indeed, in the absence of any spatio-temporal population structure, it is impossible to determine where tsetse flies captured in one particular trap came from.

In conclusion, due to the difficulties to access to all tsetse-infested zones, where multiple hosts are available for these blood feeding insects, maintaining control measures in zones frequented by human populations seems a reasonable measure, in order to protect these populations from tsetse bites and subsequent transmission of HAT, as we know that these measures are indeed very protective (Courtin et al., 2015). Given that the existence of hidden human and/or animal reservoirs can be suspected (Koffi et al., 2009; Kaboré et al., 2011; Jamonneau et al., 2012; Büscher et al., 2018), and given that we have hereby shown that the HAT focus of Boffa harbors a freely circulating tsetse population, such a measure, together

with medical surveys and treatment of infected patients, appears mandatory for now and a close future, before more research results shed more light on the eco-epidemiology of this deadly disease in mangrove ecosystems.

Appendix

Appendix 1: Information on unpublished microsatellite loci

Table A1 - Information on microsatellite loci provided by A. Robinson (Insect Pest Control Sub-program, Joint Food and Agriculture Organization of the United Nations/International Atomic Energy Agency Program of Nuclear Techniques in Food and Agriculture) used in the present study. Name of primers motif, annealing temperature (T_ann in °C), the range of sizes of amplified fragments, and primers' sequences are indicated.

Locus	Primers (5'-3')	Motif	T_ann	Size range
A10		(CA)	54.5	190
	A10F	GCAACGCCAAGTGAAATAAAG		
	A10R	TACTGGGCTCGCGTACATAAT		
B3		(GA)	55	181-195
	B3F	TTCGCTTTTGTCAGAAGTG		
	B3R	TCCCAGACGGTTCATATTAC		
XB104		(GA)	52	171-227
	B104F	ACGATTGTTCTTCTTCATTCC		
	B104R	AAGAAGCCAAACTTTCAACGCTCGC		
C102		(TGA)	52	257-278
	C102F	CGTTAAATTGTCACGATGAAG		
	C102R	AGCACATTTTTGGTACATTTATACC		

Touch-down PCR reactions were the same as in (Ségard et al., 2022):

Acknowledgements

The authors would like to thank Fabien Halkett and two anonymous referees for their comments that helped improve our manuscript. Preprint version 2 of this article has been peer reviewed and recommended by PCI Infections (https://doi.org/10.24072/pci.infections.100191; Nana Djeunga, 2024).

Funding

This work was funded by the Bill & Melinda Gates Foundation (http://www.gatesfoundation.org, grant agreement INV-001785)" and the JEAI RECIT (#400982/00) of the IRD.

Conflict of interest disclosure

The authors declare that they comply with the PCI rule of having no financial conflicts of interest in relation to the content of the article.

Author contributions

Moise S. Kagbadouno: data collection, data analyses and manuscript correction.
Modou Séré: genotyping, data analyses and manuscript correction.

Adeline Ségard: genotyping and manuscript correction.
Abdoulaye Dansy Camara: data collection and manuscript correction.
Mamadou Camara: supervision and manuscript correction.
Bruno Bucheton: supervision, data collection and manuscript correction.
Jean-Mathieu Bart: supervision, data collection and manuscript correction.
Fabrice Courtin: supervision, data collection and manuscript correction.
Thierry de Meeûs: supervision, data analyses, writing of the manuscript and design of figures.
Sophie Ravel: supervision, genotyping and manuscript correction.

Data, scripts, code, and supplementary information availability

Raw data are available on Zenodo (https://doi.org/10.5281/zenodo.8181166; Kagbadouno et al., 2023). For data analyses, all R scripts used are inserted in the main text. For other analyses we used facilities without the need of scripts (e.g. click and point programs or packages).

References

Baker MD, Krafsur ES (2001) Identification and properties of microsatellite markers in tsetse flies *Glossina morsitans* sensu lato (Diptera: Glossinidae). Molecular Ecology Notes, 1, 234–236. https://doi.org/10.1046/j.1471-8278.2001.00087.x

Balloux F (2004) Heterozygote excess in small populations and the heterozygote-excess effective population size. Evolution, 58, 1891–900. https://doi.org/10.1554/03-692

Belkhir K, Borsa P, Chikhi L, Raufaste N, Bonhomme F (2004) GENETIX 4.05, logiciel sous Windows TM pour la génétique des populations. Laboratoire Génome, Populations, Interactions, CNRS UMR 5000, Université de Montpellier II, Montpellier (France). https://kimura.univ-montp2.fr/genetix/

Benjamini Y, Yekutieli D (2001) The control of the false discovery rate in multiple testing under dependency. The Annals of Statistics, 29, 1165–1188. https://doi.org/10.1214/aos/1013699998

Berté D, De Meeus T, Kaba D, Séré M, Djohan V, Courtin F, N'Djetchi KM, Koffi M, Jamonneau V, Ta BTD, Solano P, N'Goran EK, Ravel S (2019) Population genetics of *Glossina palpalis palpalis* in sleeping sickness foci of Côte d'Ivoire before and after vector control. Infection Genetics and Evolution, 75, 103963. https://doi.org/10.1016/j.meegid.2019.103963

Bouyer J, Balenghien T, Ravel S, Vial L, Sidibé I, Thévenon S, Solano P, De Meeûs T (2009) Population sizes and dispersal pattern of tsetse flies: rolling on the river? Molecular Ecology, 18, 2787–2797. https://doi.org/10.1111/j.1365-294X.2009.04233.x

Bouyer J, Dicko AH, Cecchi G, Ravel S, Guerrini L, Solano P, Vreysen MJB, De Meeûs T, Lancelot R (2015) Mapping landscape friction to locate isolated tsetse populations candidate for elimination. Proceedings of the National Academy of Sciences of the United States of America, 112, 14575–14580. https://doi.org/10.1073/pnas.1516778112

Bouyer J, Ravel S, Dujardin JP, De Meeûs T, Vial L, Thévenon S, Guerrini L, Sidibe I, Solano P (2007) Population structuring of *Glossina palpalis gambiensis* (Diptera: Glossinidae) according to landscape fragmentation in the Mouhoun river, Burkina Faso. Journal of Medical Entomology, 44, 788–795. https://doi.org/10.1093/jmedent/44.5.788

Bucheton B, Kheir MM, El-Safi SH, Hammad A, Mergani A, Mary C, Abel L, Dessein A (2002) The interplay between environmental and host factors during an outbreak of visceral leishmaniasis in eastern Sudan. Microbes and Infection, 4, 1449–1457. https://doi.org/10.1016/s1286-4579(02)00027-8

Büscher P, Bart JM, Boelaert M, Bucheton B, Cecchi G, Chitnis N, Courtin D, Figueiredo LM, Franco JR, Grébaut P, Hasker E, Ilboudo H, Jamonneau V, Koffi M, Lejon V, MacLeod A, Masumu J, Matovu E, Mattioli R, Noyes H, Picado A, Rock KS, Rotureau B, Simo G, Thévenon S, Trindade S, Truc P, Van Reet N (2018) Do cryptic reservoirs threaten gambiense-sleeping sickness elimination? Trends in Parasitology, 34, 197–207. https://doi.org/10.1016/j.pt.2017.11.008

Camara O, Biéler S, Bucheton B, Kagbadouno M, Mathu Ndung'u J, Solano P, Camara M (2021) Accelerating elimination of sleeping sickness from the Guinean littoral through enhanced screening in the post-Ebola

context: A retrospective analysis (G Caljon, Ed,). PLOS Neglected Tropical Diseases, 15, e0009163. https://doi.org/10.1371/journal.pntd.0009163

Camara M, Caro-Riano H, Ravel S, Dujardin JP, Hervouet JP, De Meeûs T, Kagbadouno MS, Bouyer J, Solano P (2006) Genetic and morphometric evidence for population isolation of *Glossina palpalis gambiensis* (Diptera : Glossinidae) on the Loos islands, Guinea. Journal of Medical Entomology, 43, 853–860. https://doi.org/10.1093/jmedent/43.5.853

Chapuis MP, Estoup A (2007) Microsatellite null alleles and estimation of population differentiation. Molecular Biology and Evolution, 24, 621–631. https://doi.org/10.1093/molbev/msl191

Coombs JA, Letcher BH, Nislow KH (2008) CREATE: a software to create input files from diploid genotypic data for 52 genetic software programs. Molecular Ecology Resources, 8, 578–580. https://doi.org/10.1111/j.1471-8286.2007.02036.x

Cornuet JM, Luikart G (1996) Description and power analysis of two tests for detecting recent population bottlenecks from allele frequency data. Genetics, 144, 2001–2014. https://doi.org/10.1093/genetics/144.4.2001

Courtin F, Camara M, Rayaisse JB, Kagbadouno M, Dama E, Camara O, Traore IS, Rouamba J, Peylhard M, Somda MB, Leno M, Lehane MJ, Torr SJ, Solano P, Jamonneau V, Bucheton B (2015) Reducing human-tsetse contact significantly enhances the efficacy of sleeping sickness active screening campaigns: a promising result in the context of elimination. PLoS Neglected Tropical Diseases, 9. https://doi.org/10.1371/journal.pntd.0003727

Courtin F, Jamonneau V, Camara M, Camara O, Coulibaly B, Diarra A, Solano P, Bucheton B (2010) A geographical approach to identify sleeping sickness risk factors in a mangrove ecosystem. Tropical Medicine & International Health, 15, 881–889. https://doi.org/10.1111/j.1365-3156.2010.02559.x

Courtin F, Kagbadouno M (2011) Peuplements, mobilités et paysages en zone de mangrove guinéenne : le cas de la baie de Sangaréah (Guinée). Les Cahiers d'Outre-Mer, 256, 453–466. https://doi.org/10.4000/com.6358

De Meeûs T (2018) Revisiting FIS, FST, Wahlund effects, and Null alleles. Journal of Heredity, 109, 446–456. https://doi.org/10.1093/jhered/esx106

De Meeûs T, Chan CT, Ludwig JM, Tsao JI, Patel J, Bhagatwala J, Beati L (2021) Deceptive combined effects of short allele dominance and stuttering: an example with *Ixodes scapularis*, the main vector of Lyme disease in the U.S.A. Peer Community Journal, 1, e40. https://doi.org/10.24072/pcjournal.34

De Meeûs T, Guégan JF, Teriokhin AT (2009) MultiTest V.1.2, a program to binomially combine independent tests and performance comparison with other related methods on proportional data. BMC Bioinformatics, 10, 443. https://doi.org/10.1186/1471-2105-10-443

De Meeûs T, Humair PF, Grunau C, Delaye C, Renaud F (2004) Non-Mendelian transmission of alleles at microsatellite loci: an example in *Ixodes ricinus*, the vector of Lyme disease. International Journal for Parasitology, 34, 943–950. https://doi.org/10.1016/j.ijpara.2004.04.006

De Meeûs T, Lehmann L aurent, Balloux F (2006) Molecular epidemiology of clonal diploids: A quick overview and a short DIY (do it yourself) notice. Infection Genetics and Evolution, 6, 163–170. https://doi.org/10.1016/j.meegid.2005.02.004

De Meeûs T, McCoy KD, Prugnolle F, Chevillon C, Durand P, Hurtrez-Boussès S, Renaud F (2007) Population genetics and molecular epidemiology or how to "débusquer la bête." Infection Genetics and Evolution, 7, 308–332. https://doi.org/10.1016/j.meegid.2006.07.003

De Meeûs T, Noûs C (2022) A simple procedure to detect, test for the presence of stuttering, and cure stuttered data with spreadsheet programs. Peer Community Journal, 2, e52. https://doi.org/10.24072/pcjournal.165

De Meeûs T, Noûs C (2023) A new and almost perfectly accurate approximation of the eigenvalue effective population size of a dioecious population: comparisons with other estimates and detailed proofs. Peer Community Journal, 3, e51. https://doi.org/10.24072/pcjournal.280

De Meeûs T, Ravel S, Solano P, Bouyer J (2019) Negative density dependent dispersal in tsetse flies: a risk for control campaigns? Trends in Parasitology, 35, 615–621. https://doi.org/10.1016/j.pt.2019.05.007

Dempster AP, Laird NM, Rubin DB (1977) Maximum likelihood from incomplete data via the EM algorithm. Journal of the Royal Statistical Society Series B, 39, 1–38. https://doi.org/10.1111/j.2517-6161.1977.tb01600.x

Do C, Waples RS, Peel D, Macbeth GM, Tillett BJ, Ovenden JR (2014) NeEstimator v2: re-implementation of software for the estimation of contemporary effective population size (Ne) from genetic data. Molecular Ecology Resources, 14, 209–214. https://doi.org/10.1111/1755-0998.12157

Fox J (2005) The R commander: a basic statistics graphical user interface to R. Journal of Statistical Software, 14, 1–42. https://doi.org/10.18637/jss.v014.i09

Fox J (2007) Extending the R commander by "plug in" packages. R News, 7, 46–52. https://stat.ethz.ch/pipermail/r-help/attachments/20071101/3603125e/attachment.pdf

Goudet J (1995) FSTAT (Version 1.2): A computer program to calculate F-statistics. Journal of Heredity, 86, 485–486. https://doi.org/10.1093/oxfordjournals.jhered.a111627

Goudet J (2003) Fstat (ver. 2.9.4), a program to estimate and test population genetics parameters. Available at http://www.t-de-meeus.fr/Programs/Fstat294.zip, Updated from Goudet (1995).

Goudet J, De Meeûs T, Day AJ, Gliddon CJ (1994) The different levels of population structuring of dogwhelks, *Nucella lapillus*, along the south Devon coast. In: Genetics and Evolution of Aquatic Organisms (ed Beaumont A), pp. 81–95. Chapman and Hall, London.

Goudet J, Raymond M, De Meeûs T, Rousset F (1996) Testing differentiation in diploid populations. Genetics, 144, 1933–1940. https://doi.org/10.1093/genetics/144.4.1933

Holmes P (2014) First WHO meeting of stakeholders on elimination of gambiense human african trypanosomiasis. PLoS Neglected Tropical Diseases, 8, e3244. https://doi.org/10.1371/journal.pntd.0003244

Jamonneau V, Ilboudo H, Kabore J, Kaba D, Koffi M, Solano P, Garcia A, Courtin D, Laveissiere C, Lingue K, Buscher P, Bucheton B (2012) Untreated human infections by *Trypanosoma brucei gambiense* are not 100% Fatal. PLoS Neglected Tropical Diseases, 6, e1691. https://doi.org/10.1371/journal.pntd.0001691

Jamonneau V, Truc P, Grébaut P, Herder S, Ravel S, Solano P, De Meeus T (2019) *Trypanosoma brucei gambiense* group 2: the unusual suspect. Trends in Parasitology, 35, 983–995. https://doi.org/10.1016/j.pt.2019.09.002

Jones OR, Wang JL (2010) COLONY: a program for parentage and sibship inference from multilocus genotype data. Mol Ecol Resour, 10, 551–555. https://doi.org/10.1111/j.1755-0998.2009.02787.x

Jorde PE, Ryman N (2007) Unbiased estimator for genetic drift and effective population size. Genetics, 177, 927–935. https://doi.org/10.1534/genetics.107.075481

Kaboré J, Koffi M, Bucheton B, MacLeod A, Duffy C, Ilboudo H, Camara M, De Meeûs T, Belem AMG, Jamonneau V (2011) First evidence that parasite infecting apparent aparasitemic serological suspects in human African trypanosomiasis are *Trypanosoma brucei gambiense* and are similar to those found in patients. Infection Genetics and Evolution, 11, 1250–1255. https://doi.org/10.1016/j.meegid.2011.04.014

Kagbadouno MS, Camara M, Rouamba J, Rayaisse JB, Traoré IS, Camara O, Onikoyamou MF, Courtin F, Ravel S, De Meeûs T, Bucheton B, Jamonneau V, Solano P (2012) Epidemiology of sleeping sickness in boffa (Guinea): where are the trypanosomes? PLoS Neglected Tropical Diseases, 6, e1949. https://doi.org/10.1371/journal.pntd.0001949

Kagbadouno MS, Séré M, Ségard A, Abdoulaye Dansy Camara, Bucheton B, Bart J-M, Courtin F, De Meeûs T, Ravel S (2023) All data for the preprint Population genetics of *Glossina palpalis gambiensis* in the sleeping sickness focus of Boffa (Guinea) before and after eight years of vector control: no effect of control despite a significant decrease of human exposure to the disease. https://doi.org/10.5281/ZENODO.8181166

Koffi M, De Meeûs T, Bucheton B, Solano P, Camara M, Kaba D, Cuny G, Ayala FJ, Jamonneau V (2009) Population genetics of *Trypanosoma brucei gambiense*, the agent of sleeping sickness in Western Africa. Proceedings of the National Academy of Sciences of the United States of America, 106, 209–214. https://doi.org/10.1073/pnas.0811080106

Koffi M, De Meeûs T, Séré M, Bucheton B, Simo G, Njiokou F, Salim B, Kaboré J, MacLeod A, Camara M, Solano P, Belem AMG, Jamonneau V (2015) Population genetics and reproductive strategies of african trypanosomes : revisiting available published data. PLoS Neglected Tropical Diseases, 9, e0003985. https://doi.org/10.1371/journal.pntd.0003985

Luna C, Bonizzoni MB, Cheng Q, Aksoy S, Zheng L (2001) Microsatellite polymorphism in Tsetse fies (Diptera: Glossinidae). Journal of Medical Entomology, 38, 376–381. https://doi.org/10.1603/0022-2585-38.3.376

Manangwa O, De Meeûs T, Grébaut P, Segard A, Byamungu M, Ravel S (2019) Detecting Wahlund effects together with amplification problems : cryptic species, null alleles and short allele dominance in *Glossina pallidipes* populations from Tanzania. Molecular Ecology Resources, 19, 757–772. https://doi.org/10.1111/1755-0998.12989

Melachio T, Simo G, Ravel S, De Meeûs T, Causse S, Solano P, Lutumba P, Asonganyi T, Njiokou F (2011) Population genetics of *Glossina palpalis palpalis* from central African sleeping sickness foci. Parasites and Vectors, 4, 140. https://doi.org/10.1186/1756-3305-4-140

Nana Djeunga H (2024) Reaching the last miles for transmission interruption of sleeping sickness in Guinea: follow-up of achievements and policy making using microsatellites-based population genetics. *Peer Community In Infections*, 100191. https://doi.org/10.24072/pci.infections.100191

Nei M, Tajima F (1981) Genetic drift and estimation of effective population size. Genetics, 98, 625–640. https://doi.org/10.1093/genetics/98.3.625

Nomura T (2008) Estimation of effective number of breeders from molecular coancestry of single cohort sample. Evolutionary Applications, 1, 462–474. https://doi.org/10.1111/j.1752-4571.2008.00015.x

Peel D, Waples RS, Macbeth GM, Do C, Ovenden JR (2013) Accounting for missing data in the estimation of contemporary genetic effective population size (N_e). Molecular Ecology Resources, 13, 243–253. https://doi.org/10.1111/1755-0998.12049

Pollak E (1983) A new method for estimating the effective population size from allele frequency changes. Genetics, 104, 531–548. https://doi.org/10.1093/genetics/104.3.531

Pudovkin AI, Zaykin DV, Hedgecock D (1996) On the potential for estimating the effective number of breeders from heterozygote excess in progeny. Genetics, 144, 383–387. https://doi.org/10.1093/genetics/144.1.383

Ravel S, De Meeûs T, Dujardin JP, Zeze DG, Gooding RH, Dusfour I, Sane B, Cuny G, Solano P (2007) The tsetse fly *Glossina palpalis palpalis* is composed of several genetically differentiated small populations in the sleeping sickness focus of Bonon, Côte d'Ivoire. Infection Genetics and Evolution, 7, 116–125. https://doi.org/10.1016/j.meegid.2006.07.002

Ravel S, Mahamat MH, Ségard A, Argiles-Herrero R, Bouyer J, Rayaisse J-B, Solano P, Mollo BG, Pèka M, Darnas J, Belem AMG, Yoni W, Noûs C, De Meeûs T (2023) Population genetics of *Glossina fuscipes* fuscipes from southern Chad. Peer Community Journal, 3, e31. https://doi.org/10.24072/pcjournal.257

Ravel S, Sere M, Manangwa O, Kagbadouno M, Mahamat MH, Shereni W, Okeyo WA, Argiles-Herrero R, De Meeûs T (2020) Developing and quality testing of microsatellite loci for four species of *Glossina*. Infection Genetics and Evolution, 85, 104515. https://doi.org/10.1016/j.meegid.2020.104515

R-Core-Team (2022) R: A Language and Environment for Statistical Computing. http://www.R-project.org

Robertson A (1965) The interpretation of genotypic ratios in domestic animal populations. Animal Production, 7, 319–324. https://doi.org/10.1017/S0003356100025770

Ségard A, Romero A, Ravel S, Truc P, Dobigny G, Gauthier P, Etougbetche J, Dossou H-J, Badou S, Houéménou G, Morand S, Chaisiri K, Noûs C, De Meeûs T (2022) Development of nine microsatellite loci for *Trypanosoma lewisi*, a potential human pathogen in Western Africa and South-East Asia, and preliminary population genetics analyses. Peer Community Journal, 2, e69. https://doi.org/10.24072/pcjournal.188

Simarro PP, Cecchi G, Franco JR, Paone M, Diarra A, Priotto G, Mattioli RC, Jannin JG (2015) Monitoring the Progress towards the Elimination of Gambiense Human African Trypanosomiasis. PLoS Neglected Tropical Diseases, 9, e0003785. https://doi.org/10.1371/journal.pntd.0003785

Solano P, Duvallet G, Dumas V, Cuisance D, Cuny G (1997) Microsatellite markers for genetic population studies in *Glossina palpalis* (Diptera: Glossinidae). Acta Tropica, 65, 175–180. https://doi.org/10.1016/S0001-706X(97)00663-3

Solano P, Ravel S, Bouyer J, Camara M, Kagbadouno MS, Dyer N, Gardes L, Herault D, Donnelly MJ, De Meeûs T (2009) The population structure of *Glossina palpalis gambiensis* from island and continental locations in coastal Guinea. PLoS Neglected Tropical Diseases, 3, e392. https://doi.org/10.1371/journal.pntd.0000392

Vitalis R, Couvet D (2001a) Estimation of effective population size and migration rate from one- and two-locus identity measures. Genetics, 157, 911–925. https://doi.org/10.1093/genetics/157.2.911

Vitalis R, Couvet D (2001b) ESTIM 1.0: a computer program to infer population parameters from one- and two-locus gene identity probabilities. Molecular Ecology Notes, 1, 354–356. https://doi.org/10.1046/j.1471-8278.2001.00086.x

Wang JL (2009) A new method for estimating effective population sizes from a single sample of multilocus genotypes. Molecular Ecology, 18, 2148–2164. https://doi.org/10.1111/j.1365-294X.2009.04175.x

Wang JL, Whitlock MC (2003) Estimating effective population size and migration rates from genetic samples over space and time. Genetics, 163, 429–446. https://doi.org/10.1093/genetics/163.1.429

Waples RS, Do C (2010) Linkage disequilibrium estimates of contemporary Ne using highly variable genetic markers: a largely untapped resource for applied conservation and evolution. Evolutionary Applications, 3, 244–262. https://doi.org/10.1111/j.1752-4571.2009.00104.x

Weir W, Capewell P, Foth B, Clucas C, Pountain A, Steketee P, Veitch N, Koffi M, De Meeûs T, Kaboré J, Camara M, Cooper A, Tait A, Jamonneau V, Bucheton B, Berriman M, MacLeod A (2016) Population genomics reveals the origin and asexual evolution of human infective trypanosomes. eLife, 5, e11473. https://doi.org/10.7554/eLife.11473

Weir BS, Cockerham CC (1984) Estimating F-statistics for the analysis of population structure. Evolution, 38, 1358–1370. https://doi.org/10.1111/j.1558-5646.1984.tb05657.x

Williams BG (1990) Tsetse fly (Diptera: Glossinidae) population dynamics and the estimation of mortality rates from life-table data. Bulletin of Entomological Research, 80, 479–485. http://dx.doi.org/10.1017/S0007485300050756

Wright S (1965) The interpretation of population structure by F-statistics with special regard to system of mating. Evolution, 19, 395–420. https://doi.org/10.1111/j.1558-5646.1965.tb01731.x